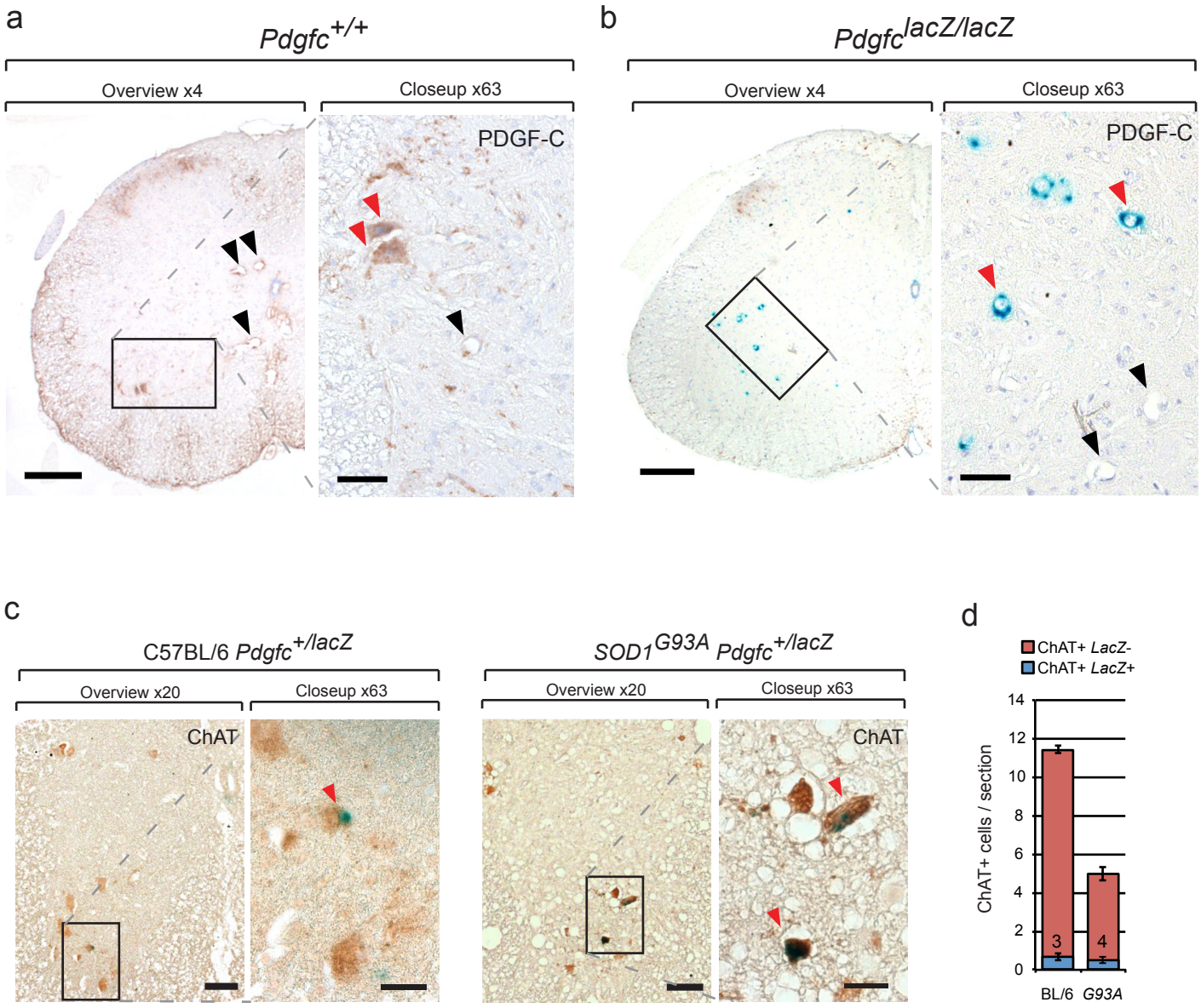

Supplementary Figure 1.

Location of PDGF-C protein and transcript in mouse spinal cord. (**a**) PDGF-C immunostaining in *Pdgfc*$^{+/+}$ mice is indicating neuron-resembling cells as source of expression (red arrowheads) with some staining around vessels (black arrowheads). Bar for overview: 200 µm, closeup: 20 µm in panels a and b. (**b**) Sections from *Pdgfc*$^{lacZ/lacZ}$ mice stained for PDGF-C simultaneously with sections from panel A show neuronal cells (red arrowheads) but not vessels (black arrowheads) as source of recombinant beta-galactosidase activity and lack of non-specific anti-PDGF-C antibody binding. (**c**) Colocalization of LacZ activity in *Pdgfc*$^{+/lacZ}$ mice within a group of neuronal cells expressing ChAT. Bar for overview: 50 µm, closeup: 20 µm. Histochemistry staining target in panels a, b and c is indicated in the upper right corner. (**d**) Number of LacZ-positive cells in *Pdgfc*$^{+/lacZ}$ mice within neuronal population expressing ChAT (n shown above axis label).

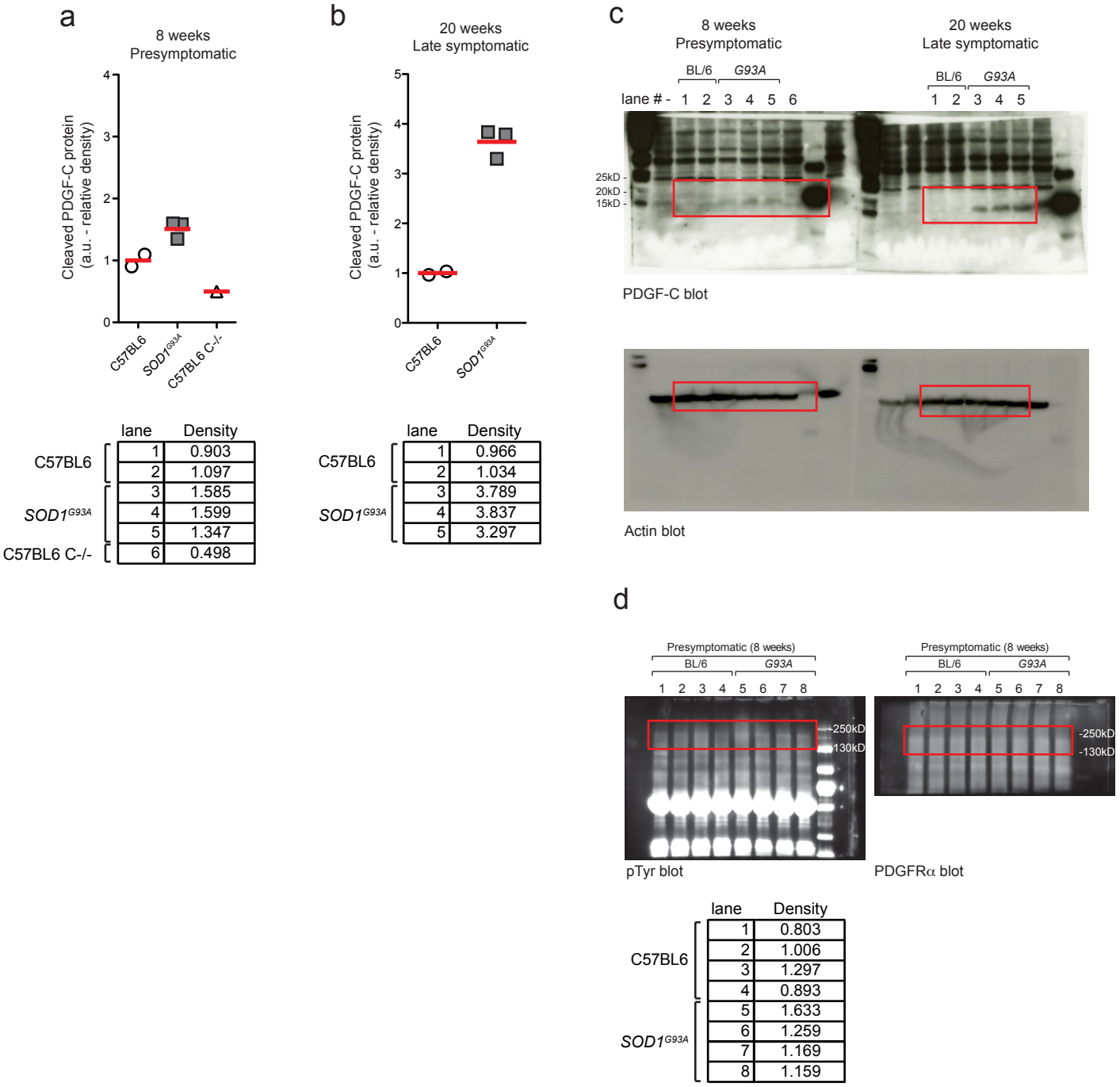

	lane	Density
C57BL6	1	0.903
	2	1.097
SOD1^{G93A}	3	1.585
	4	1.599
	5	1.347
C57BL6 C-/-	6	0.498

	lane	Density
C57BL6	1	0.966
	2	1.034
SOD1^{G93A}	3	3.789
	4	3.837
	5	3.297

	lane	Density
C57BL6	1	0.803
	2	1.006
	3	1.297
	4	0.893
SOD1^{G93A}	5	1.633
	6	1.259
	7	1.169
	8	1.159

Supplementary Figure 2

Densitometry quantifications and western blotting. (**a**) PDGF-C protein expression detected in presymptomatic *SOD1*^{G93A} mice and (**b**) late-symptomatic *SOD1*^{G93A} mice. (**c**) Uncropped blots for the PDGF-C and actin proteins in figure 1f. Cropped areas are marked with red boxes. (**d**) Uncropped blots for pTyr and PDGFRα in figure 1g. Cropped areas are marked with red boxes. Normalised density values from respective lanes are presented in tables below the graphs.

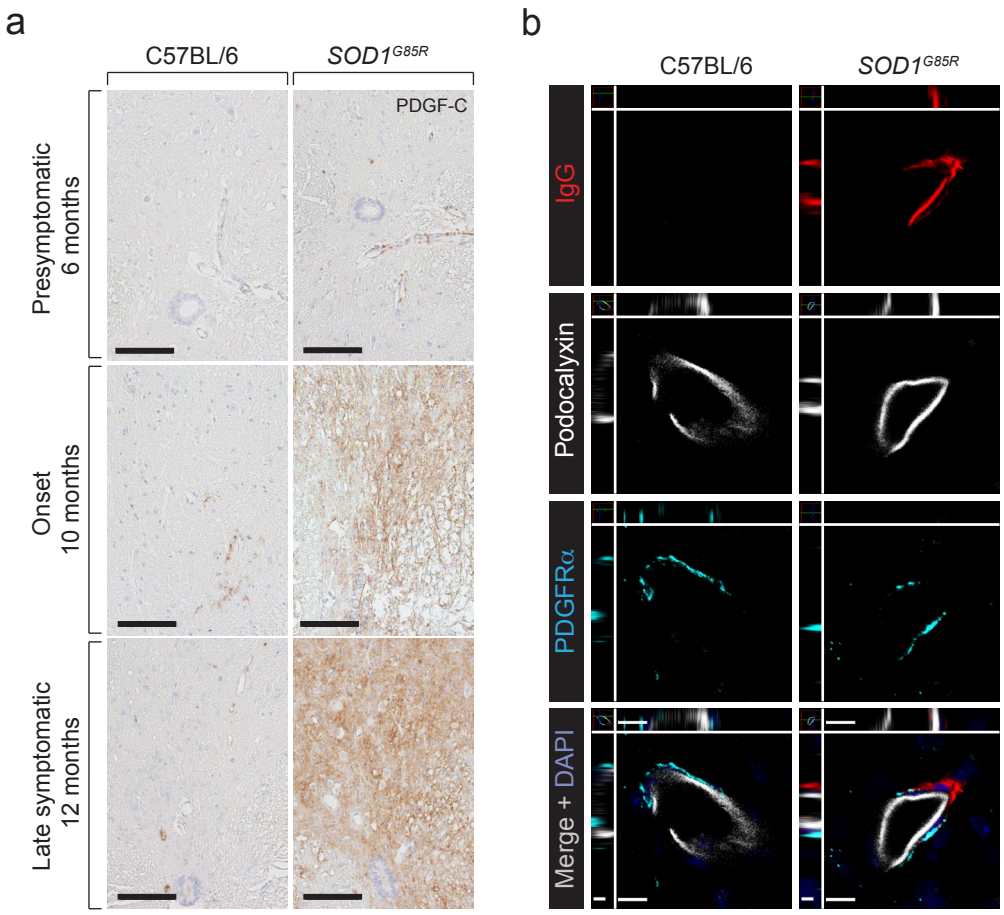

Supplementary Figure 3

Accumulation of PDGF-C and BSCB deregulation in PDGFRα positive vessels in *SOD1^{G85R}* mice with inactive SOD1. (**a**) Accumulation of PDGF-C protein as determined by immunohistochemistry during disease progression in presymptomatic (6 months), onset (10 months) and late symptomatic phase (12 months) in *SOD1^{G85R}* mice. Staining target is indicated in the upper right corner. Bar: 100 µm. (**b**) Vessels in presymptomatic (6 months) *SOD1^{G85R}* mice are displaying IgG uptake (red) and are surrounded with perivascular astrocytes expressing PDGFRα (turquoise). Vessel lumen is stained with podocalyxin (white). Bar: 10 µm.

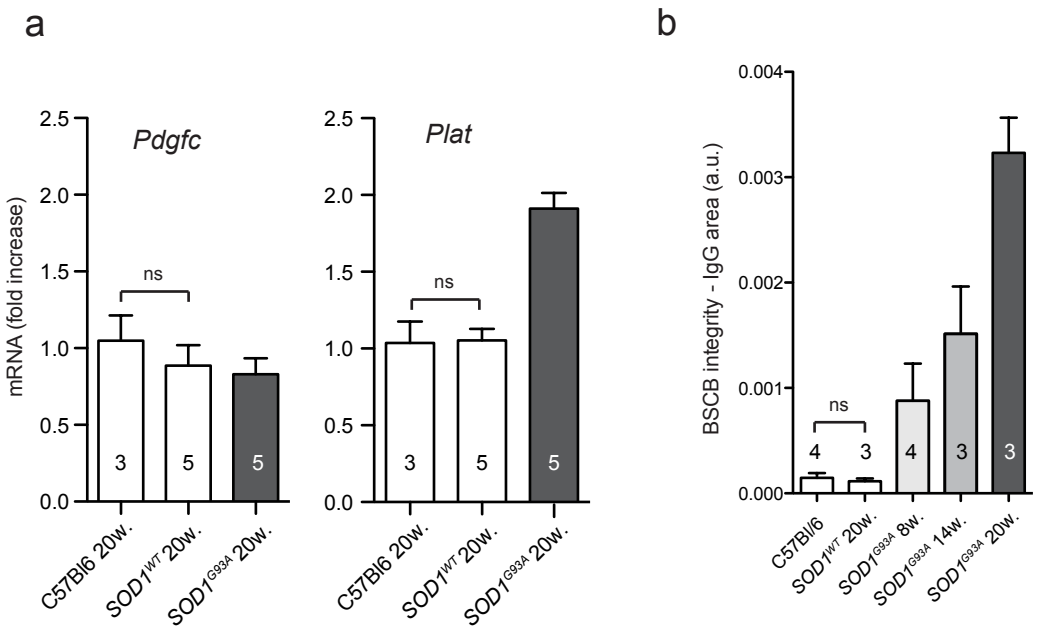

Supplementary Figure 4

***SOD1^{WT}* mice do not show activation of the PDGF-CC pathway or BSCB deregulation.** (**a**) Quantification of mRNA expression for *Pdgfc* and *Plat* (tPA) in *SOD1^{WT}* and *SOD1^{G93A}* mice (n shown above label). Mean ± s.e.m, two-tailed t-test. (**b**) Quantification of BSCB dysfunction shown by IgG area immunofluorescence from lumbar region sections (n shown above label). Mean ± s.e.m, two-tailed Mann-Whitney test.

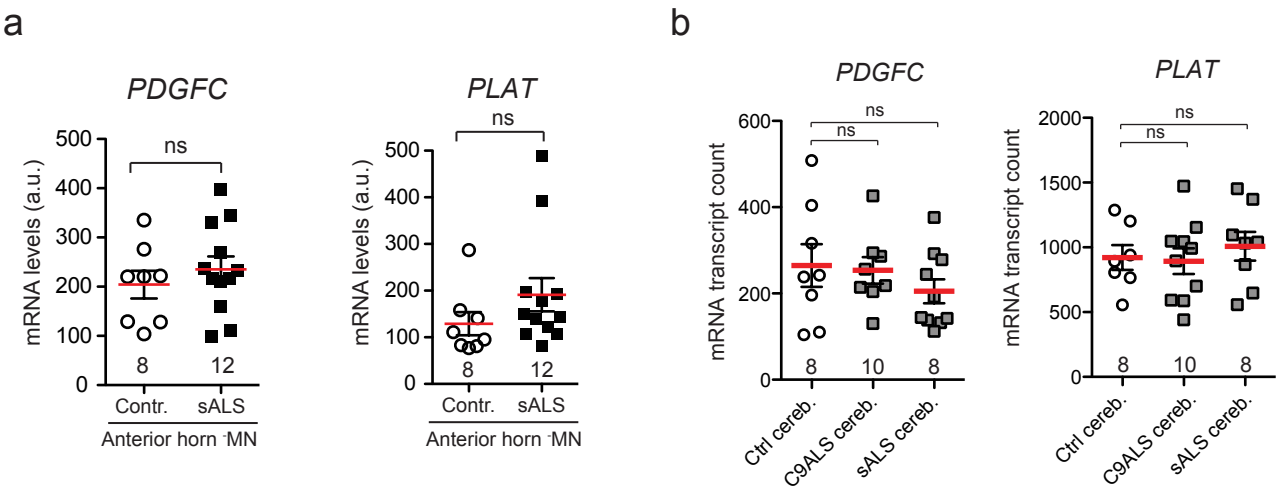

Supplementary Figure 5

mRNA expression levels for *PLAT* (tPA) and *PDGFC* in the anterior horn after laser captured excision of motoneurons (**a**) and in the cerebellum (**b**) of sporadic human ALS, *C9Orf72* ALS and control subjects (n shown above axis label). Mean ± s.e.m, two-tailed t-test.

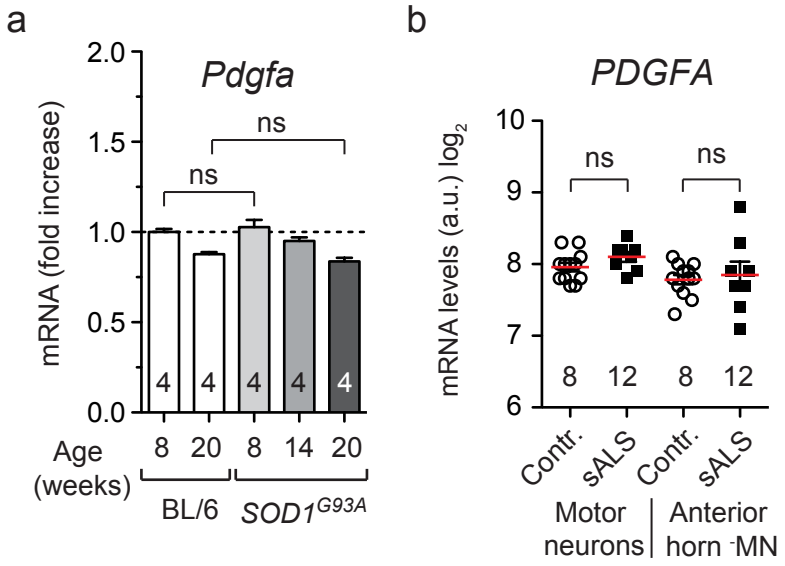

Supplementary Figure 6

Expression of *PDGFA* in ALS. (**b**) mRNA expression of *Pdgfa* in *SOD1*^{G93A} mice (n shown above label). (**b**) mRNA expression of *PDGFA* in motor neuron (MN) and anterior horn (AH) spinal cord fractions of sporadic human ALS (n=12). Mean ± s.e.m, two-tailed t-test.

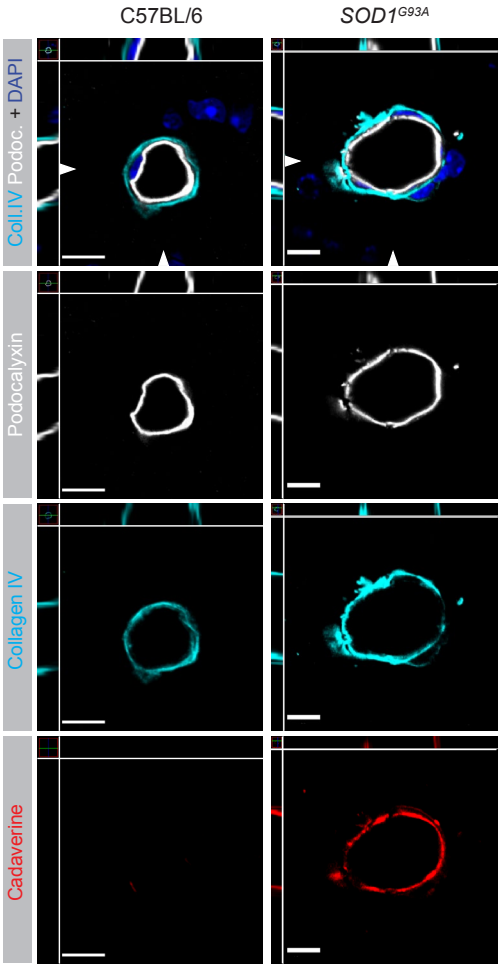

Supplementary Figure 7

Correct polarization of endothelial cells in vessels showing BSCB dysfunction in 14 week old *SOD1^{G93A}* mice. Basement membrane is shown with immunostaining for collagen IV (turquoise) and luminal EC membrane is outlined with staining for podocalyxin (white). Barrier dysfunction is indicated with cadaverine A555 tracer (red). Z stack cross-section location is shown with arrowheads. Bar: 10 µm.

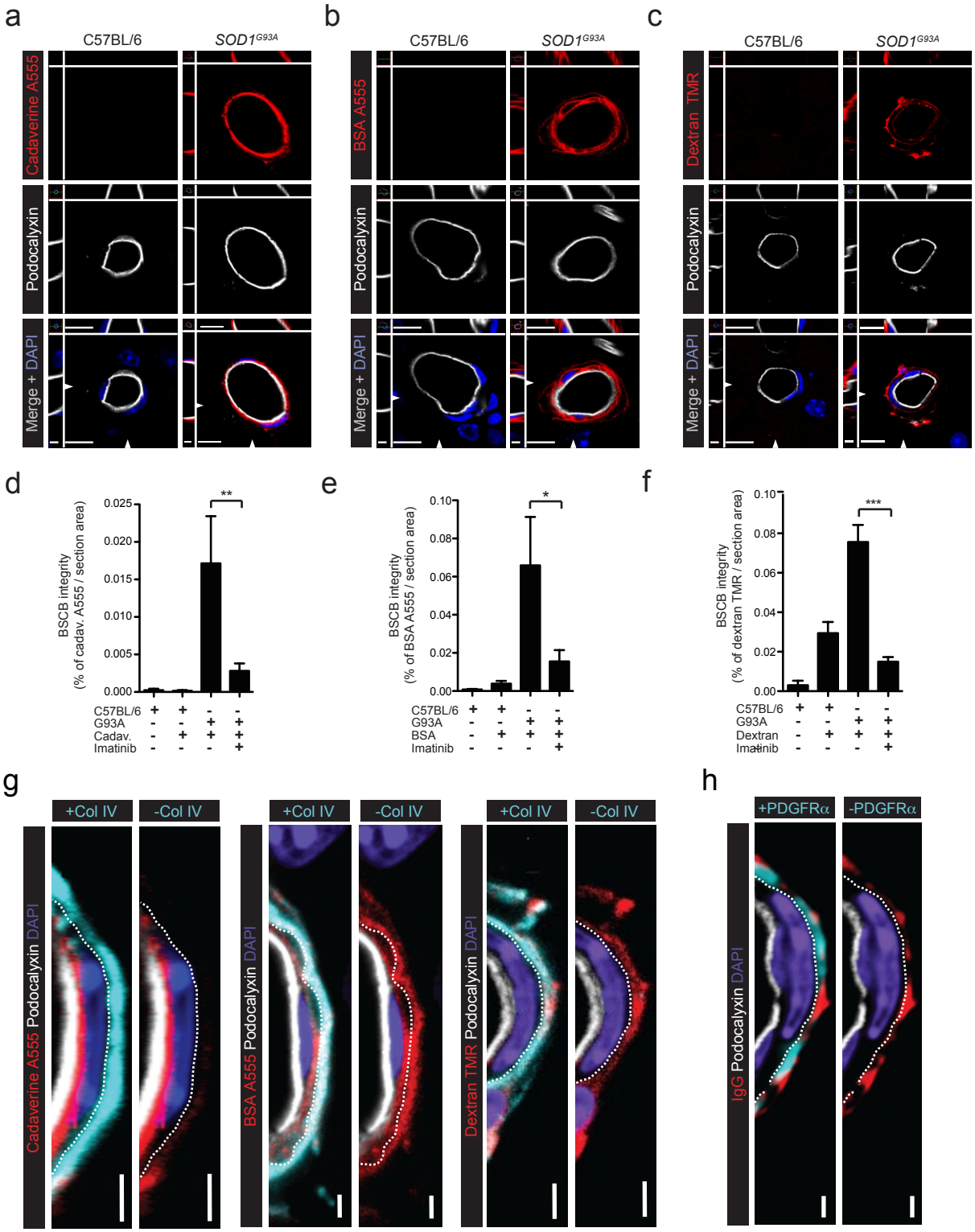

Supplementary Figure 8

Inhibition of PDGF-CC signalling with imatinib decreases endothelial uptake of molecular tracers in *SOD1^{G93A}* mice. (**a**, **b**, **c**) Vascular uptake patterns of exogenous fluorescence-labelled tracers in 14 week old C57BL/6 and *SOD1^{G93A}* mice in relation to the EC luminal membrane counterstained with podocalyxin (white). (**a**) Cadaverine Alexa 555 (red) accumulated within EC at 2 h post injection. (**b**) BSA Alexa 555 (red) colocalized within EC area at 16 h post injection. (**c**) Dextran TMR 70kD (red) observed in EC and vascular periphery at 16 h post injection. Z stack cross-section location is shown with arrowheads. Bar: 10 µm. (**d**, **e**, **f**) Quantification of tracer uptake area in 14 w. old C57BL/6 and *SOD1^{G93A}* mice after 7 day pretreatment with PBS or imatinib (150 mg/kg/day). (**d**) Cadaverine Alexa 555 (n=4, **p=0.008), (**e**) BSA Alexa 555 (n=4, *p=0.046), (**f**) Dextran TMR (n=3, ***p=0.0001). Mean ± s.e.m, two-tailed Mann-Whitney test. (**g**, **h**) Location of exogenous and endogenous markers in spinal cord vessels of symptomatic *SOD1^{G93A}* mice. (**g**) Location of Cadaverin A555, BSA A555 or Dextran TMR (red) in relation to endothelial cells. Luminal EC membrane is outlined with podocalyxin staining (white) and abluminal membrane is outlined with Collagen IV staining (turquoise). The endothelial - abluminal interface is marked with white dotted line. (**h**) Location of endogenous IgG in relation to astrocyte endfeet outlined with PDGFRα staining (turquoise). The interface between abluminal membrane and astrocyte endfeet is marked with white dotted line. Pictures represent single confocal microscopy z-sections. Bar: 2 µm

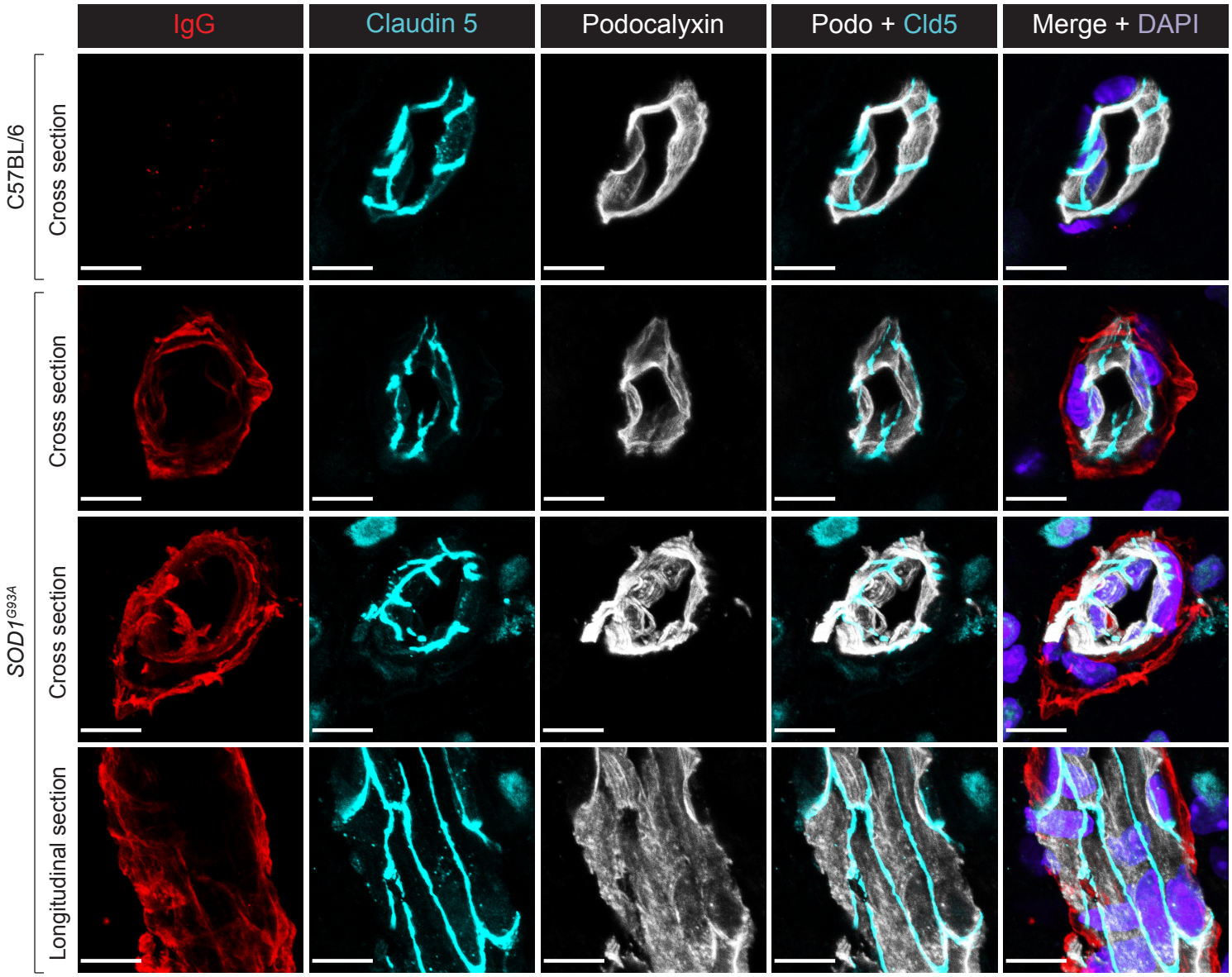

Supplementary Figure 9

Presence of tight junctions in vessels with BSCB dysfunction in symptomatic *SOD1^{G93A}* mice. Immunoglobulin (IgG - red) uptake is observed in 20 week old *SOD1^{G93A}* spinal cord vessels where tight junctions (claudin 5 - cyan) are present between endothelial cells. Endothelial luminal membrane is outlined with podocalyxin staining (white). The image is a maximum intensity projection of 10 confocal images representing 10 µm thick tissue section. Bar: 10 µm.

		Gehan-Breslow--Wilcoxon	Log rank (Mantel-Cox)
Disease onset	Gender - balanced *SOD1*^{G93A} *C+/+* (n=32, 107.5d) vs. *C-/-* (n=23, 121d)	p=0.0001	p=0.0003
	Females *SOD1*^{G93A} *C+/+* (n=14, 107.5d) vs. *C-/-* (n=13, 119d)	p=0.028	p=0.107
	Males *SOD1*^{G93A} *C+/+* (n=18, 102d) vs. *C-/-* (n=10, 123d)	p=0.0017	p=0.0001
	Gender - balanced *SOD1*^{G93A} *C+/+* (n=32, 107.5d) vs. *C+/-* (n=33, 119d)	p=0.0001	p=0.0002
	Females *SOD1*^{G93A} *C+/+* (n=14, 107.5d) vs. *C+/-* (n=17, 117d)	p=0.03	p=0.17
	Males *SOD1*^{G93A} *C+/+* (n=18, 102d) vs. *C+/-* (n=16, 122d)	p=0.001	p=0.0002
	SOD1^{G93A} PBS (n=17, 106d) vs. Imatinib (n=19, 117d)	p=0.052	p=0.056

Supplementary Figure 10

Table presenting p-values for compared onset estimates between *Pdgfc* allele, treatment types, gender and survival tests.

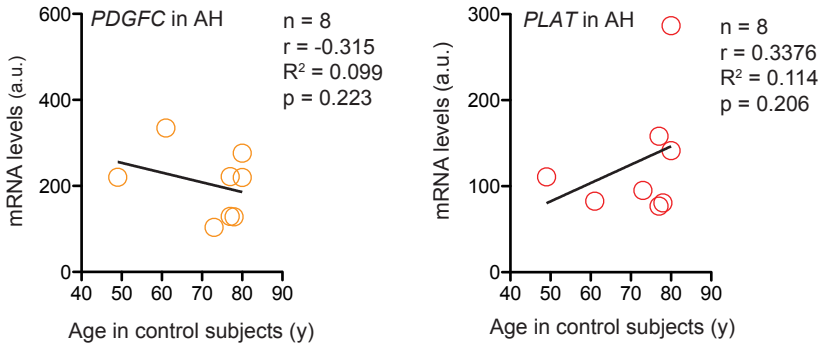

Supplementary Figure 11

Lack of correlation between age and mRNA expression of *PDGFC* or *PLAT* in anterior horn (AH) in control subjects. r - Pearsons' correlation, R2 - coefficient of determination, p - t-test p-value.

a

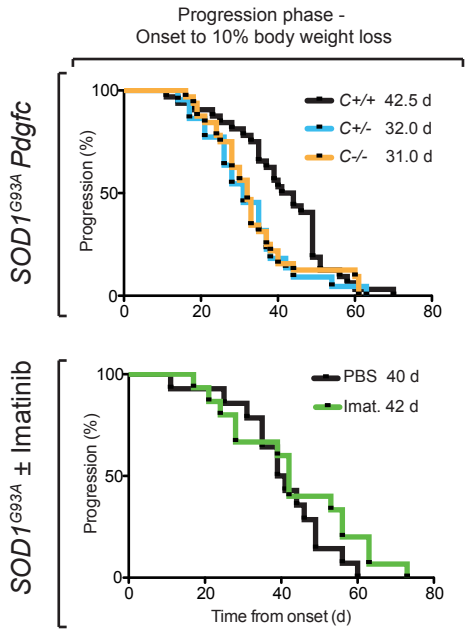

b

		Gehan-Breslow--Wilcoxon	Log rank (Mantel-Cox)
Progression	*SOD1*^{G93A} C+/+ (n=32, 42.5d) vs. C-/- (n=23, 31d)	p=0.007	p=0.016
	SOD1^{G93A} C+/+ (n=32, 42.5d) vs. C+/- (n=33, 32d)	p=0.01	p=0.06
	SOD1^{G93A} PBS (n=14, 40d) vs. Imatinib (n=15, 42d)	p=0.063	p=0.24

c

		Gehan-Breslow--Wilcoxon	Log rank (Mantel-Cox)
Progression to endpoint	*SOD1*^{G93A} C+/+ (n=29, 17d) vs. C-/- (n=23, 6d)	p=0.0001	p=0.0001
	SOD1^{G93A} C+/+ (n=29, 17d) vs.C+/- (n=27, 9.5d)	p=0.001	p=0.001
	SOD1^{G93A} PBS (n=11, 17d) vs. Imatinib (n=15, 10d)	p=0.0553	p=0.028
Endpoint	*SOD1*^{G93A} C+/+ (n=29, 161d) vs. C-/- (n=23, 159.5d)	p=0.37	p=0.19
	SOD1^{G93A} C+/+ (n=29, 161d) vs.C+/- (n=27, 159d)	p=0.51	p=0.51
	SOD1^{G93A} PBS (n=11, 169d) vs. Imatinib (n=15, 170d)	p=0.49	p=0.95

Supplementary Figure 12

Event estimates of disease progression. (a) *SOD1*^{G93A}*Pdgfc*$^{+/+}$ (n=32) or *SOD1*^{G93A} PBS-treated mice (black, n=17) are compared to *SOD1*^{G93A}*Pdgfc*$^{-/-}$ (orange, n=23), *SOD1*^{G93A}*Pdgfc*$^{+/-}$ (turquoise, n=33) and *SOD1*^{G93A} treated with 100mg/kg/day imatinib from the age of 8 weeks (green, n=19). Median event values are shown in legends. (**b**) Table presenting p-values for respective cohorts and intervention types at progression phase using Log rank (Mantel-Cox) and Gehan-Breslow-Wilcoxon tests. (**c**) Table presenting p-values for respective cohorts and intervention types at progression to endpoint and overall survival from birth to endpoint using Log rank (Mantel-Cox) and Gehan-Breslow-Wilcoxon tests.

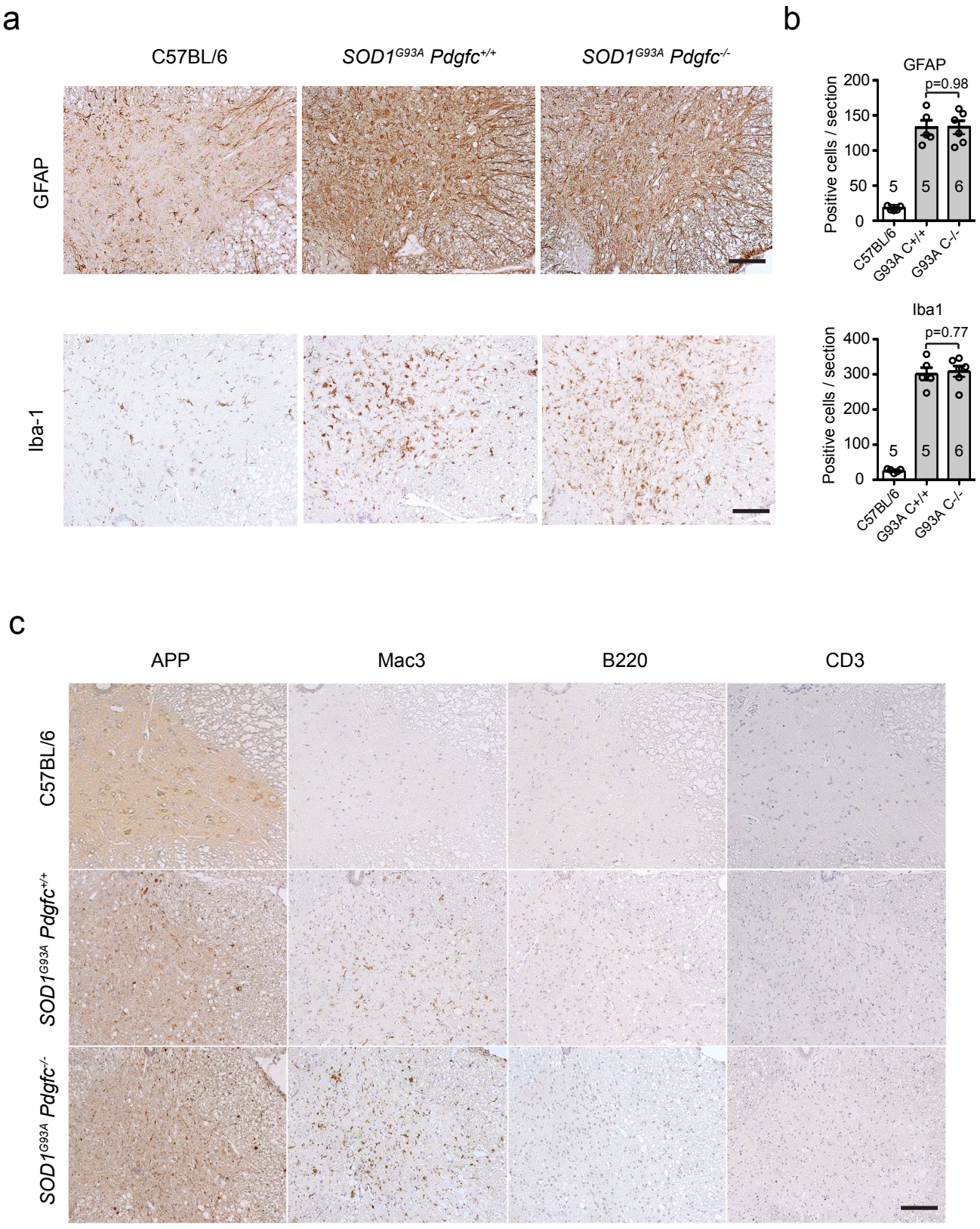

Supplementary Figure 13

Neuroinflammation in late symptomatic *SOD1^{G93A} Pdgfc$^{+/+}$* and *SOD1^{G93A} Pdgfc$^{-/-}$* mice. (**a**) Immunostainings for GFAP and Iba-1 markers in spinal cord overview (bar 100 µm). (**b**) Quantifications of cells stained with GFAP and Iba-1. p values for two-tailed t-test are shown above brackets (n shown above axis label). (**c**) Macrophage (Mac-3), B-cell (B220) and T-cell (CD3) marker immunohistochemistry stainings in late symptomatic *SOD1^{G93A} Pdgfc$^{+/+}$* and *SOD1^{G93A} Pdgfc$^{-/-}$* mice. Neuronal cells on adjacent sections are visualized with amyloid precursor protein (APP) for histological reference (bar 100 µm).